ADVANCED MATERIALS
www.advmat.de

Full Control and Manipulation of Heat Signatures: Cloaking, Camouflage and Thermal Metamaterials

*Tiancheng Han, Xue Bai, John T. L. Thong, Baowen Li, and Cheng-Wei Qiu**

An object can be perceived and identified due to its unique scattering signature in various physical fields, e.g., optics, electromagnetics, acoustics, thermotics, etc. Analogous to wave-dynamic illusion, thermal camouflage can potentially transform an actual perception into a pre-controlled perception, thus empowering unprecedented applications in thermal cloaking and illusion. In this paper, we propose and realize a functional thermal camouflage device, which is capable of creating multiple expected images off the original object's position in heat conduction. The thermal scattering signature of the object is thus metamorphosed and perceived as multiple ghost targets with different geometries and compositions. The thermal camouflage effect is experimentally confirmed in both time-dependent and temperature-dependent cases, demonstrating excellent thermodynamic performance, which may open a new avenue to control the diffusive heat flow in ways inconceivable with phonons.

Manipulation of various physical fields, including optics, electromagnetics, acoustics, thermotics, etc, has been a long-standing dream for many researchers over the decades. Recently, many significant achievements have been motivated by pioneering theoretical works.[1–4] With the rapid development of technologies and artificial materials, invisibility cloaks have been experimentally demonstrated both at optical[5,6] and RF[7–9] frequencies. Decoupling electric and magnetic effects, dc magnetic cloak[10,11] and dc electric cloak[12,13] have been experimentally realized using ferromagnetic-superconductor materials and resistor networks, respectively. Beyond controlling electromagnetic/dc fields,[1–13] the theoretical tool of coordinate transformation has been extended to the other areas of physics, such as acoustics[14,15] matter waves[16] elastic waves,[17] and heat flux.[18–21]

In contrast to invisibility that changes an arbitrary object into nothing[1–21] illusion usually refers to the change of signatures for one object into another in a specific physical field[22–28] Optical illusion was first proposed based on double-negative complementary materials,[22] and has been experimentally demonstrated in composite transmission-line RLC circuits.[23] The planar RLC circuits based illusion device is inherently restricted to lumped circuitry on a circuit board. Soon after, wave-dynamic experiments on radar illusion were demonstrated,[24,25] which can only simply reduce the apparent size or change the effective material property of the original object. Recently, we reported a radar ghost illusion device using microwave metamaterials,[26] which can not only reduce the apparent size and change the effective material property of the original object, but can also alter and shift the scattering center of the original object. Beyond optical illusion,[22–26] based on the same coordinate transformation theory,[1] dc illusion[27] and acoustic illusion[28] have been experimentally realized by using resistor networks and anisotropic metamaterials, respectively.

In this paper, we report a meaningful functional camouflage device in thermotics, which transforms the thermal scattering signature of an arbitrary object to that of multiple isolated expected objects. In other words, the functional device can make the thermal scattering signature of the "cloaked" object equivalent to that of multiple other objects. Different from the previous transformation-optics-based proposals that needs complicated metamaterial design,[22–28] thus leading to many practical limitations, our thermal camouflage device is designed based on an exact bilayer cloak that only employs naturally-occuring materials. In an actual experimental setup, the proposed device is carefully investigated in both time-dependent and temperature-dependent cases, demonstrating excellent thermodynamic performance.

The evolution and functions from thermal cloaking to thermal camouflage are schematically illustrated in the left column of **Figure 1**. In a heat conduction field, an exposed "man" can be unambiguously detected from his thermal signature, as shown in Figure 1a1. When the "man" is covered by a thermal cloak (see Figure 1b1, the corresponding thermal signature vanishes, which means that you can not detect the existence of the "man". However, when the "man" is shrouded by the designed device (see Figure 1c1, the corresponding thermal signature is completely different from that of Figure 1a1, but exactly the same as that of two "women" in Figure 1d1. Therefore, with the camouflage device, what you can "see" or "feel"

Dr. T. Han, X. Bai, Prof. J. T. L. Thong,
Prof. C.-W. Qiu
Department of Electrical and Computer Engineering
National University of Singapore
117583, Republic of Singapore
E-mail: ELEQC@nus.edu.sg
X. Bai, Prof. J. T. L. Thong, Prof. B. Li,
Prof. C.-W. Qiu
NUS Graduate School for Integrative Sciences and Engineering
National University of Singapore
Kent Ridge, 117456, Republic of Singapore
X. Bai, Prof. B. Li
Department of Physics and Centre for Computational Science and Engineering, National University of Singapore
Singapore, 117546, Republic of Singapore
Prof. B. Li
Center for Phononics and Thermal Energy Science
School of Physics Science and Engineering
Tongji University
200092, Shanghai, China

DOI: 10.1002/adma.201304448

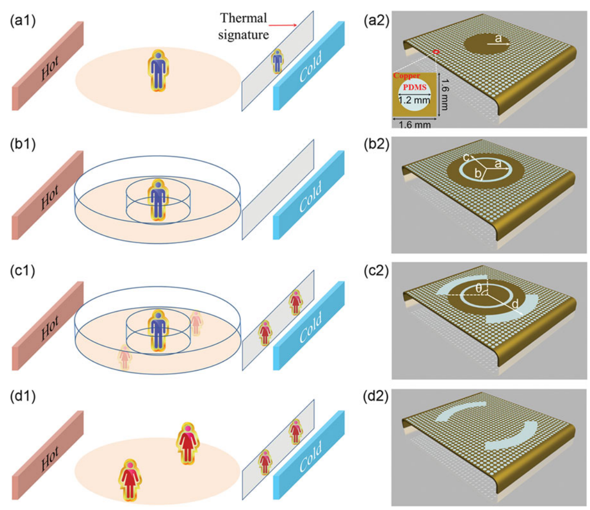

Figure 1. Evolution, function, and realization from thermal cloaking to thermal camouflage. (a) The thermal signature shows a "man" (a copper cylinder) when a bare "man" (a copper cylinder) stands in a heat conduction field. (b) The thermal signature vanishes when the "man" (the copper cylinder) is covered by a bilayer thermal cloak. (c) The "man" (the copper cylinder) shrouded by the designed camouflage device shows the metamorphosed thermal feature of the "man" (the copper cylinder), i.e. two "women" (two insulated sectors). (d) The thermal signature of two "woman" (two insulated sectors) is equivalent to the camouflage device in (c). Left column corresponds to conceptual scheme, and right column corresponds to physical realization. Geometric parameters: a = 30 mm, b = 33 mm, c = 50 mm, d = 70 mm, and θ = 90°. Inset shows the geometric size and materials of a unit cell.

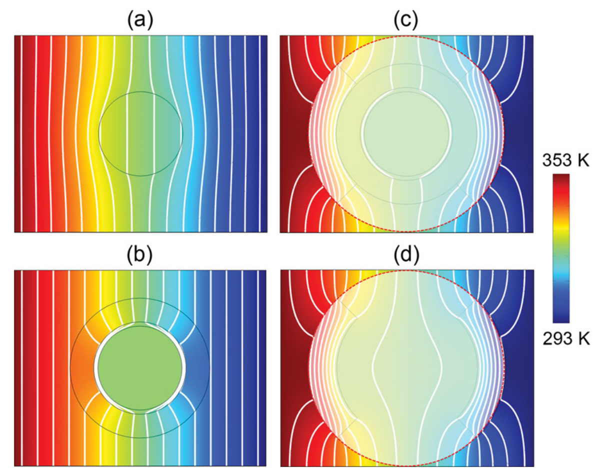

Figure 2. Simulated temperature profiles for proposed devices in Figure 1. (a) Original object (a bare copper cylinder) corresponding to Figure 1a2. (b) Bilayer thermal cloak corresponding to Figure 1b2. (c) Thermal camouflage device corresponding to Figure 1c2. (d) Equivalent objects corresponding to Figure 1c2. Isothermal lines are also represented in white color in panel. As predicted, the simulations clearly demonstrate the camouflage phenomenon in thermal scattering signatures.

is not the actual object, but rather something different. The expected objects, deliberately devised to be seen, can be predesigned and precisely controlled.

The above functionality can be derived based on a two-fold operation. The first is to eliminate the scattering of the original object by using an exact bilayer cloak, and the second is to create the desired scattering signature by placing expected objects. The bilayer thermal cloak (see in Figure 1b2) is composed of an inner layer ($a < r < b$) and an outer layer ($b < r < c$) with conductivity of κ_2 and κ_3, respectively. The conductivity of the background is κ_b. By using an inner layer that is perfectly insulating, i.e., $\kappa_2 = 0$, this ensures that an external field does not penetrate into the cloaking region and the only task then is to eliminate the external-field distortion. The external-field distortion is eliminated when $\kappa_3 = \dfrac{c^2+b^2}{c^2-b^2}\kappa_b$, which means that the third parameter can be uniquely determined if any two of κ_3, κ_b, c/b are known. Thus an exact bilayer thermal cloak is obtained, based on which a thermal camouflage device is finally formed by placing expected objects beside the bilayer cloak.

For practical realization of the bilayer cloak, the inner layer is polydimethylsiloxane (PDMS) with conductivity of κ_{PDMS} = 0.15 W m^{-1} K^{-1}, and the outer layer is copper with conductivity of κ_{Cu} = 394 W m^{-1} K^{-1}. The required conductivity of the background is achieved by drilling holes into a copper plate and filling them with PDMS. The PDMS area fraction f is obtained from the Maxwell-Garnett formula[29] $\kappa_b = \kappa_{Cu}\left[1+\dfrac{2(\kappa_{PDMS}-\kappa_{Cu})f}{\kappa_{PDMS}+\kappa_{Cu}-(\kappa_{PDMS}-\kappa_{Cu})f}\right]$. On the basis of an experimental optimization, we choose a square lattice of holes with lattice constant 1.6 mm and diameter 1.2 mm, leading to f = 44%. Thus we obtain κ_b = 156 W m^{-1} K^{-1}, and the calculated geometric parameters: a = 30 mm, b = 33 mm, c = 50 mm. The actual object (a bare copper cylinder) is shown in Figure 1a2, and the fabricated bilayer thermal cloak is schematically illustrated in Figure 1b2. By placing two expected objects beside the bilayer cloak, a thermal camouflage device is formed in Figure 1c2, in which a cloaked copper object is transformed into two PDMS wing-ghosts in the thermal scattering signature. The equivalent expected objects of the designed device are portrayed in Figure 1d2. The performance of the proposed schemes in Figure 1 is numerically verified based on a finite element method (FEM), as shown in **Figure 2**. The temperature distribution of original object (a bare copper cylinder) is demonstrated in Figure 2a. When the object is covered by the bilayer cloak in Figure 2b, the thermal scattering vanishes, demonstrating no distortion of the external fields as if there were nothing. However, when the object is shrouded by the camouflage device in Figure 2c, metamorphosing thermal signature is presented, which completely different from Figure 2a. For reference, the equivalent objects of two standalone PDMS wings are simulated in Figure 2d. The effectiveness of the camouflage device in thermal scattering signature is confirmed via the equivalence between the identical patterns in Figures 2c and 2d outside the outermost boundary (red dotted circle). In other words, the proposed device camouflages the initial thermal signature of a conductor (copper cylinder), replacing this with the expected thermal signature of two insulators (PDMS).

We fabricated the bilayer thermal cloak, camouflage device, and equivalent objects, corresponding to Figure 1b2, Figure 1c2, and Figure 1d2, respectively. In the experimental setup, local heating on the left side of the plate is achieved by immersing the lip into a tank filled with hot water (80 °C),

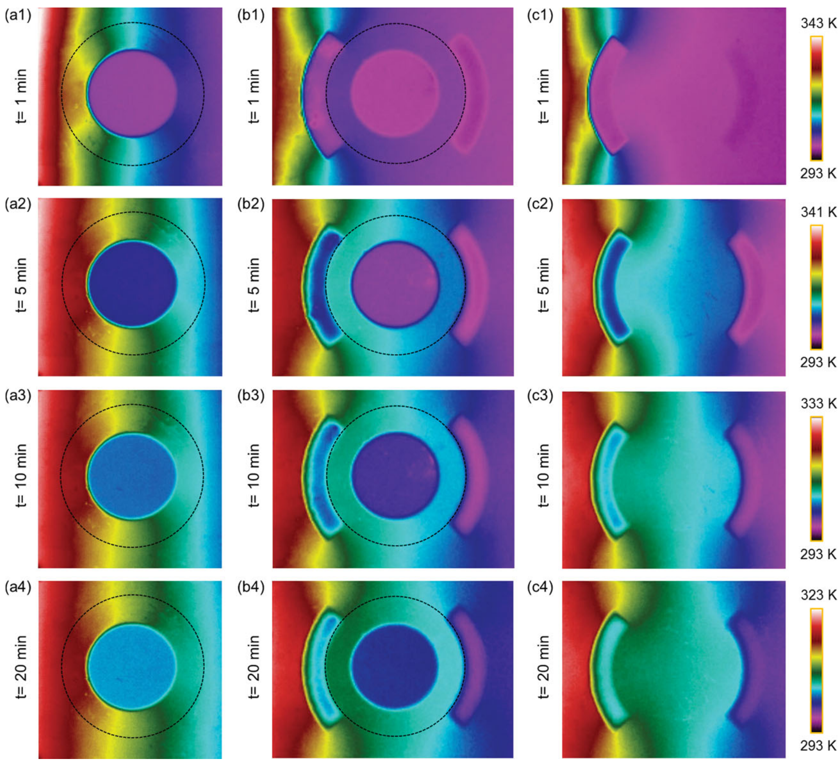

Figure 3. Experimental measurement of transient temperature profiles at different times t = 1, 5, 10, 20 min. (a) Results for the bilayer cloak in Figure 1b2. (b) Results for the camouflage device in Figure 1c2. (c) Results for the equivalent objects in Figure 1d2.Obviously, the proposed devices show excellent performance as time elapses.

while the right side is connected to a tank filled with water at room temperature. The cross-sectional temperature profile is captured with a Flir i60 infrared camera. The transient temperature distributions of the proposed devices are measured at different times t = 1, 5, 10, and 20 min after placing the left side of the sample into hot water (80 °C). The measured result of the bilayer cloak is shown in **Figure 3**a, which demonstrates its ability to maintain the heat-front and its heat protection capabilities. It is apparent that the cloak successfully fulfills its task in that the central region is colder than its surrounding by reducing the external heat flux that enters the cloaking region. Furthermore, both front and rear temperature fronts outside the cloak remain nearly planar as time elapses. The simulation results corresponding to Figure 3a are provided in Supplementary Figure S1a, in which good agreement can be seen. Figure 3b shows the measured results of the camouflage device, which accords very well with simulation results in Supplementary Figure S1b.

Figure 3b shows the measured results of the camouflage device, which accords very well with equivalent objects in Figure 3c. The simulation results of the camouflage device and corresponding expected objects are also provided in Supplementary Figures S1b and S1c, which present good agreement with the experiment results. Because our heat source is boiled water, it is noted that the temperature drops with time during the measurement. With the change of temperature, thermal signature is always maintained, demonstrating the temperature-independent property of the proposed camouflage device.

The heat baths in the simulations are mimicked by fixed temperatures, showing good agreement with measured ones, which can be further corroborated by normalizing the temperature distributions. As the inner layer of bilayer cloak is not made of a perfect thermal insulation material ($\kappa = 0$), a small amount of thermal energy will diffuse into the cloaking region and raise the temperature after a long time. Hence, thermal protection works only transiently (but over a respectable period of time as demonstrated in our thermal cloak), but the heat-front maintenance never fails as time elapses. Therefore, on the basis of exact bilayer cloak, the camouflage device retains the same thermal scattering signature as time elapses, demonstrating a thermotic camouflage effect.

To examine the omnidirectional effectiveness of the proposed camouflage device, we calculated the temperature distributions when the heat conduction is along different directions, as shown in **Figure 4**. It is concluded that the camouflage device functions equally well for arbitrary incident heat fields via the equivalence seen in the identical patterns in Figures 4a and 4b for vertical incidence, and Figures 4c and 4d for oblique incidence. It is also important to investigate the effectiveness of the camouflage effect when multiple camouflage devices are put together and mutual coupling may occur between them. The simulation results of multiple camouflage

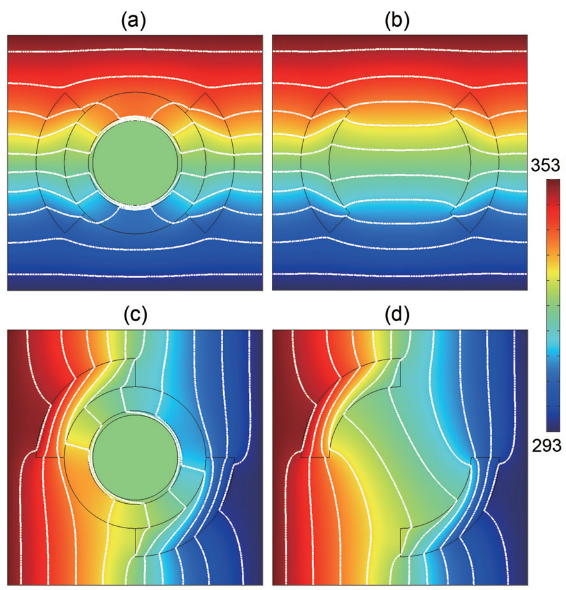

Figure 4. Temperature distributions for thermal camouflage device and corresponding expected objects with the heat conduction along different directions. (a,b) Vertical incidence. (c,d) Oblique incidence. Isothermal lines are superimposed as white lines in panel.

devices are given in Supplementary Figure S2. Clearly, both for horizontal incidence (Figures S2a and S2b)and vertical incidence (Figures S2c and S2d), the thermal scattering pattern of camouflage array agrees very well with corresponding expected objects.

In summary, we have experimentally demonstrated a thermal camouflage device enabling an object to possess arbitrary wing-ghosts off its original position and produce expected images. Our design scheme, derived directly from the conduction equation, does not rely on transformation optics,[1] and thus avoids the problems present in previous proposals, such as extreme parameters (inhomogeneous and anisotropic material properties) and complicated fabrication.[22–28] The metamorphosis of thermal signature has been verified in both time-dependent and temperature-dependent cases, which demonstrate good camouflage performance in thermotics. It should be pointed out that the work presented has introduced a new dimension to the emerging field of phononics: controlling and manipulating heat flow with phonons.[30]

Experimental Section

The bilayer camouflage device are fabricated by drilling holes into a copper plate and filling them with PDMS. On the basis of an experimental optimization, we choose a square lattice of holes with lattice constant 1.6 mm and diameter 1.2 mm. The cross-sectional temperature profile is captured with a Flir i60 infrared camera.

Supporting Information

Supporting Information is available from the Wiley Online Library or from the author.

Acknowledgements

This work was supported in part from the MINDEF-NUS JPP Grant R-263-000-A38-133 administered by National University of Singapore, in part from the National Science Foundation of China under Grant No. 11304253, and in part from the Southwest University (SWU112035).

Received: September 4, 2013
Revised: October 26, 2013
Published online: February 5, 2014

[1] J. B. Pendry, D. Schurig, D. R. Smith, *Science* **2006**, *312*, 1780.
[2] U. Leonhardt, *Science* **2006**, *312*, 1777.
[3] A. Alù, N. Engheta, *Phys. Rev. E* **2005**, *72*, 016623.
[4] A. Alù, N. Engheta, *Phys. Rev. Lett.* **2008**, *100*, 113901.
[5] J. Valentine, J. Li, T. Zentgraf, G. Bartal, X. Zhang, *Nat. Mater.* **2009**, *8*, 568.
[6] T. Ergin, N. Stenger, P. Brenner, J. B. Pendry, M. Wegener, *Science* **2010**, *328*, 337.
[7] R. Liu, C. Ji, J. J. Mock, J. Y. Chin, T. J. Cui, D. R. Smith, *Science* **2009**, *323*, 366.
[8] H. F. Ma, T. J. Cui, *Nat. Commun.* **2010**, *1*, 124.
[9] N. Landy, D. R. Smith, *Nat. Mater.* **2013**, *12*, 25.
[10] F. Gomory, M. Solovyov, J. Souc, C. Navau, J. Prat-Camps, A. Sanchez, *Science* **2012**, *335*, 1466.
[11] S. Narayana, Y. Sato, *Adv. Mater.* **2012**, *24*, 71.
[12] F. Yang, Z. L. Mei, T. Y. Jin, *Phys. Rev. Lett.* **2012**, *109*, 053902.
[13] F. Yang, Z. L. Mei, X. Y. Yang, T. Y. Jin, T. J. Cui, *Adv. Funct. Mater.* **2013**, 10.1002/adfm.201300226.
[14] S. Zhang, C. Xia, N. Fang, *Phys. Rev. Lett.* **2011**, *106*, 024301.
[15] B.-I. Popa, L. Zigoneanu, S. A. Cummer, *Phys. Rev. Lett.* **2011**, *106*, 253901.
[16] S. Zhang, D. A. Genov, C. Sun, X. Zhang, *Phys. Rev. Lett.* **2008**, *100*, 123002.
[17] M. Brun, S. Guenneau, A. B. Movchan, *Appl. Phys. Lett.* **2009**, *94*, 061903.
[18] C. Fan, Y. Gao, J. Huang, *Appl. Phys. Lett.* **2008**, *92*, 251907.
[19] J. Li, Y. Gao, J. Huang, *J. Appl. Phys.* **2010**, *108*, 074504.
[20] S. Narayana, Y. Sato, *Phys. Rev. Lett.* **2012**, *108*, 214303.
[21] R. Schittny, M. Kadic, S. Guenneau, M. Wegener, *Phys. Rev. Lett.* **2013**, *110*, 195901.
[22] Y. Lai, J. Ng, H. Chen, D. Han, J. Xiao, Z. Zhang, C. T. Chan, *Phys. Rev. Lett.* **2009**, *102*, 253902.
[23] C. Li, X. Meng, X. Liu, F. Li, G. Fang, H. Chen, C. T. Chan, *Phys. Rev. Lett.* **2010**, *105*, 233906.
[24] W. X. Jiang, T. J. Cui, *Phys. Rev. E* **2011**, *83*, 026601.
[25] W. X. Jiang, T. J. Cui, X. M. Yang, H. F. Ma, Q. Cheng, *Appl. Phys. Lett.* **2011**, *98*, 204101.
[26] W. X. Jiang, C.-W. Qiu, T. C. Han, S. Zhang, T. J. Cui, *Adv. Funct. Mater.* **2013**, 10.1002/adfm.201203806.
[27] M. Liu, Z. L. Mei, X. Ma, T. J. Cui, *Appl. Phys. Lett.* **2012**, *101*, 051905.
[28] W. Kan, B. Liang, X. Zhu, R. Li, X. Zou, H. Wu, J. Yang, J. Cheng, *Sci. Rep.* **2013**, 10.1038/srep01427.
[29] J. C. Maxwell-Garnett, *Philos. Trans. R. Soc. London* **1904**, *203*, 385.
[30] N. B. Li, J. Ren, L. Wang, P. Huang, B. Li, *Rev. Mod. Phys.* **2012**, *84*, 1045.